JCTC Journal of Chemical Theory and Computation

Article

Cite This: J. Chem. Theory Comput. 2018, 14, 3289−3297

pubs.acs.org/JCTC

Membrane-Induced pK_a Shifts in *wt*-pHLIP and Its L16H Variant

Diogo Vila-Viçosa,[†,§] Tomás F. D. Silva,[†,§] Gregory Slaybaugh,[‡] Yana K. Reshetnyak,[‡] Oleg A. Andreev,[‡] and Miguel Machuqueiro*[,†]

[†]Centro de Química e Bioquímica, BioISI: Biosystems and Integrative Sciences Institute, Departamento de Química e Bioquímica, Faculdade de Ciências, Universidade de Lisboa, 1749-016 Lisboa, Portugal

[‡]Department of Physics, University of Rhode Island, 2 Lippitt Road, Kingston, Rhode Island 02881, United States

Supporting Information

ABSTRACT: The pH (low) insertion peptides (pHLIPs) is a family of peptides that are able to insert into a lipid bilayer at acidic pH. The molecular mechanism of pHLIPs insertion, folding, and stability in the membrane at low pH is based on multiple protonation events, which are challenging to study at the molecular level. More specifically, the relation between the experimental pK of insertion (pK^{exp}) of pHLIPs and the pK_a of the key residues is yet to be clarified. We carried out a computational study, complemented with new experimental data, and established the influence of (de)protonation of titrable residues on the stability of the peptide membrane-inserted state. Constant-pH molecular dynamics simulations were employed to calculate the pK_a values of these residues along the membrane normal. In the *wt*-pHLIP, we identified Asp14 as the key residue for the stability of the membrane-inserted state, and its pK_a value is strongly correlated with the experimental pK^{exp} measured in thermodynamics studies. Also, in order to narrow down the pH range at which pHLIP is stable in the membrane, we designed a new pHLIP variant, L16H, where Leu in the 16th position was replaced by a titrable His residue. Our results showed that the L16H variant undergoes two transitions. The calculated pK_a and experimentally observed pK^{exp} values are in good agreement. Two distinct pK^{exp} values delimit a pH range where the L16H peptide is stably inserted in the membrane, while, outside this range, the membrane-inserted state is destabilized and the peptide exits from the bilayer. pHLIP peptides have been successfully used to target cancer cells for the delivery of diagnostics and therapeutic agents to acidic tumors. The fine-tuning of the stability of the pHLIP inserted state and its restriction to a narrow well-defined pH range might allow the design of new peptides, able to discriminate between tissues with different extracellular pH values.

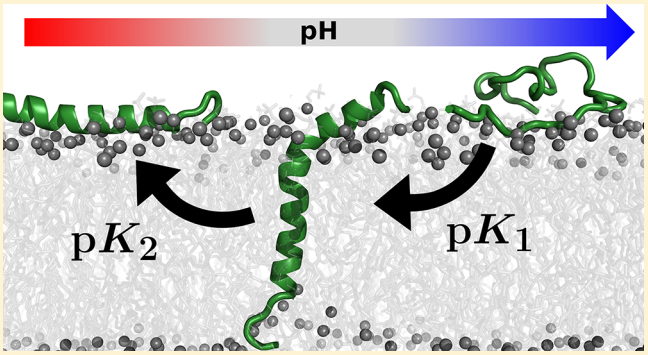

1. INTRODUCTION

The pH (low) insertion peptides (pHLIPs) is a family of peptides that insert into lipid bilayers at low pH.[1−8] The original version of this peptide was derived from a transmembrane C helix of bacteriorhodopsin.[1] Biophysical studies revealed three major states of pHLIPs (see Figure 1 in ref 9): (State I) when the peptide is in solution and does not adopt a defined structure; (State II) in the presence of a membrane at neutral or high pH the peptide is mostly unstructured yet adsorbed to the bilayer surface (pHLIPs with different sequences adopt different configurations in this state[10,11]); finally (State III), by lowering pH, the key residues protonate, leading to an increase of the peptide hydrophobicity and insertion across the membrane to form a stable transmembrane (TM) α-helix.[3] This behavior from pHLIP peptides is significantly different from other typical transmembrane peptides, such as the WALP/KALP peptide family.[12−16] In this case, the high membrane affinities are pH-independent and lead to inserted transmembrane helical structures, even when ionized residues are introduced in the middle of the WALP sequence.[16,17]

pHLIP sequences share common features: a TM region, with hydrophobic residues and one or more acids (Asp or Glu), and N- and C-terminus flanking sequences. Both flanking sequences have several charged residues, which are essential for peptide solubility. In most pHLIPs, C-terminus flanking sequences are transient membrane inserting segments[18], which contain a variable number of anionic groups, affecting the rate of pHLIP insertion/withdrawal from the bilayer.[5] The TM sequence (WARYA^{14}DWLFTTPLLLL^{25}DLALLV) of wild-type (*wt*) pHLIP contains many hydrophobic residues (including two Trp residues, which are used to monitor the propagation of the peptide into the lipid bilayer) and two Asp residues at positions 14 and 25. These titrable residues play an essential role in both the pH-dependent insertion of pHLIP into the lipid bilayer and the stability of the membrane-inserted state, since they must be

Received: January 31, 2018
Published: May 7, 2018

DOI: 10.1021/acs.jctc.8b00102
J. Chem. Theory Comput. 2018, 14, 3289−3297

protonated (at least partially) for the insertion process to occur.[19] Thermodynamics studies of Trp fluorescence changes in pHLIP with pH on liposomes allow for investigation of the stability of the membrane-inserted state at different pH values, which is typically presented by a pK of the peptide insertion (pK_{ins} − onward referred to as pK^{exp}). This pK value is expected to be related with the pK_a of one or both Asp residues at the membrane/water interface. In fact, the pK^{exp} of the *wt*-pHLIP is 6.0,[20] which is the expected value for Asp at the interface.[21] Moreover, pHLIP peptides with single mutations D14E or D25E (Asp−> Glu) show an increase in the pK^{exp} of ∼0.5 pK units,[20] which is approximately the difference in the pK_a values between Asp and Glu in solution. This suggests that the pK_a values of these acids are strongly related with pK^{exp}. The effect of shifting Asp14 to the 13th or 15th positions, which, in principle, changes the solvent exposure of this residue, has also been studied.[22] These results, where the pK^{exp} decrease is concomitant with an increase of solvent exposure (13th position) and vice versa,[22] suggest a crucial role of Asp14 in the stability of the membrane-inserted state.

A typical pHLIP variant has a single value of pK^{exp}: a pH below which more than 50% of the peptide population is inserted in the bilayer. Since acidosis is a universal marker for tumor identification, the pH-sensitive interaction of pHLIPs with the cell membrane renders it a good transport system for tumor targeting, delivering drugs, and imaging agents to cancer cells. pHLIP can target and accumulate in tissues with the extracellular pH below pK^{exp}, usually cancer cells in tumors, but also naturally acidic organs, such as kidneys and stomach (in the case of oral administration).[20,23,24] It would be advantageous to control the stability of pHLIP's inserted state and restrict it to a narrow well-defined pH range. Cationic residues, when protonated (charged), have been shown to hinder pHLIP membrane insertion.[23] A histidine residue, when inserted in a lipid bilayer, has its pK_a value shifted below the pK_a of aspartic acid,[21] leading to a protonation event (generation of a positive charge), which could destabilize the membrane-inserted state and induce the peptide withdrawal from the membrane. In theory, it requires a large enough difference between the His and Asp pK_a values to generate a significant population of the inserted peptide (where His and Asp are in their neutral forms) but narrow enough to allow the peptide to discriminate between organs/tumors with slightly different acidities.

The investigation of the protonation states of the titrable residues in pHLIPs is an essential step in understanding the molecular mechanism of pHLIP action and might open an opportunity to design new peptide variants with desirable targeting properties. Computational approaches are well suited to address this challenge. In particular, molecular dynamics (MD) simulations have been used to investigate the membrane insertion mechanism[25,26] and the stability of pHLIP.[27] However, in classical MD simulations all protonation states are fixed, which means that pH is not explicitly modeled. Constant-pH molecular dynamics (CpHMD) methods[21,28−51] have been developed over the years to allow the inclusion of pH effects in MD simulations. In the stochastic titration method, the Poisson−Boltzmann estimated energies are used in Monte Carlo calculations to obtain protonation states that are representative of the system conformation/configuration. The use of continuum electrostatics to obtain the free energies of changing protonation states has been successfully adopted by many methods,[21,30−45] while offering the important advantage of computational speed. We have extended the stochastic titration method[30,34] to include lipid bilayers (CpHMD-L)[43,44] in order to study the protonation profiles of peptides and proteins interacting with lipid bilayers.[21] This methodology was recently used to calculate the pK_a values of individual titrable amino acids when inserting in a lipid bilayer and showed that, despite sampling limitations, it was possible to estimate pK_a values at deep inserted positions, right before losing contact with bulk water, hence with the proton buffer.[21]

Here, we used our recently developed CpHMD-L method to study the protonation profile of all titrable amino acids in pHLIP when inserted in a lipid bilayer (State III). These simulations were performed to identify the key residues determining the stability of pHLIP in the membrane, which is reflected by the observed experimental pK^{exp}. We also proposed a new pHLIP sequence with a histidine located near the key Asp14 (L16H pHLIP variant). Computer simulations predicted a second protonation event at lower pH values, that experimental results confirmed to be also related with a peptide withdrawal from the membrane.

2. METHODS

2.1. System Setup and CpHMD Simulations. In this work, we focused our efforts on the *wt* sequence of pHLIP[24] and L16H variant (see Table 1). In the case of L16H variant,

Table 1. pHLIP Sequences Used in This Work[a]

variant	sequence
wt	ACEQNPIYWARYA^{14}DWLFTTPLLLL^{25}DLALLVDADEGT
L16H	ACEQNPIYWARYA^{14}DWHFTTPLLLL^{25}DLALLVDADEGT

[a]Asp14 and His16 positions are underlined.

we replaced the Leu residue at the 16th position with a His since, being two positions below Asp14 in a α-helical structure, the two residues should point to opposite directions. The rationale is based on the assumption that these residues do not interact strongly, thus, they should have their pK_a values only weakly correlated.

The *wt* and L16H pHLIP sequences were simulated using the stochastic titration CpHMD-L method.[21,30,34,43,44] The peptides were built inserted in a bilayer of 256 2-oleoyl-1-palmitoyl-*sn*-glycero-3-phosphocholine (POPC) lipid molecules and placed with Asp14 and Asp25, in their protonated (neutral) forms, equidistant to the membrane center. This unbiased configuration was chosen to avoid favoring the solvent exposure of one acidic residue over the other. The protonation states of Asp, Glu, His, Cys, C-ter, and N-ter were allowed to titrate in the pH range of 4.0 to 7.0, with a 1.0 pH step. Each CpHMD cycle was 20 ps long (τ_{prt}), and each solvent relaxation step was 0.2 ps long (τ_{rlx}). At each pH value, five replicates were performed for 100 ns. Within this short time scale, the peptides are expected to remain inserted in the membrane which allows us to characterize the pH effects on the membrane-inserted state of pHLIP (State III). The first 20 ns were disregarded in the analyses to allow for system equilibration.

2.2. Molecular Dynamics Settings. All molecular dynamics simulations were performed with the GROMOS 54A7 force field[52] using a modified version[34] of GROMACS 4.0.7.[53] A twin-range scheme was used with short- and long-range cutoffs of 8 and 14 Å, respectively, with neighbor lists between the two cutoff values being updated every 5 steps. Long-range electrostatic interactions were treated with the

DOI: 10.1021/acs.jctc.8b00102
J. Chem. Theory Comput. 2018, 14, 3289−3297

generalized reaction field (RF) method.[54] Although the RF method is not optimal to capture the long-range electrostatics of membrane systems, due to its anisotropic nature, there are several advantages in its use within the CpHMD framework, namely the high computation speed and its consistency with the recent GROMOS force fields (including lipid parameters),[55] where all parametrization and validation were performed with this method. Recently, it has been shown that the system net charge can introduce systematic errors in pK_a values obtained with a λ-dynamics based CpHMD method.[56] However, with our CpHMD method, which uses GRF and an implicit ionic strength in the protonation calculations (see below), we have not observed such effects.[34,45]

The RF dielectric constant used was 54,[57] and an ionic strength of 0.1 M was also employed. The lipid and protein bond lengths were constrained using the P-LINCS algorithm,[58] while the SETTLE algorithm[59] was used for water molecules (simple point charge, SPC[60]). Newton equations of motion were integrated using a time step of 2 fs keeping constant the number of molecules, the pressure, and the temperature (NPT ensemble). The temperature of the systems was separately coupled to a v-rescale[61] temperature bath at 310 K and relaxation times of 0.1 ps. A semi-isotropic Parrinello−Rahman pressure coupling[62] was used at 1 bar with a relaxation time of 5 ps and a compressibility of 4.5×10^{-5} bar^{-1}.

2.3. Poisson−Boltzmann/Monte Carlo Calculations. The Poisson−Boltzmann (PB) calculations were performed using the program DelPhi V5.1,[63] using partial charges from the GROMOS 54A7 and radii obtained from the Lennard-Jones parameters of this force field. These calculations were performed on the fully atomistic pHLIP/POPC system. The molecular surface of the solute (here the solute can be seen as the membrane + peptide supramolecular complex) was defined using a probe of radius 1.4 Å, the ion exclusion layer was 2.0 Å, and the ionic strength was 0.1 M. A dielectric constant of 2 was used for the solute and 80 for the solvent. A two step focusing procedure was used with grid spacing of approximately 1 and 0.25 Å in the large and small grids, respectively (corresponding to 91 grid points). In the coarse grid, relaxation parameters of 0.20 and 0.75 were used in the linear and nonlinear iterations processes, and periodic boundary conditions were applied in the x and y directions. The background interactions were calculated up to 25 Å, and the convergence threshold for the electrostatic potential was set to 0.01.

The PB-derived free energy terms were then used to sample protonation states within a Monte Carlo (MC) scheme performed using the PETIT program.[64] Proton tautomerism was taken into account in all titrable groups. 10^5 MC cycles were performed for each conformation where a cycle corresponds to a trial change of each individual site.

2.4. pK_a Calculation along the Membrane Normal. To calculate the residues pK_a values along the membrane normal, we split our conformations according to their relative depth to the average position of membrane "P" atoms within a 6 Å radius from pHLIP. This method describes better the local deformations induced by the peptide, since it only uses neighboring "P" atoms to obtain the reference average position.

After sorting the conformations in 1 Å insertion slices, we separate them by protonation states of the group of interest. Here, we apply a minimum criteria of 50 frames in at least 2 pH values in order to be able to calculate the pK_a values and estimate their standard errors. The protonation states in each slice are used in a Hill fitting procedure to obtain the respective pK_a value.

Assuming that a peptide stability in the membrane is regulated by the protonation of a single titrable residue, then the most inserted pK_a value of this residue can be regarded as our "in silico" estimation of the experimentally measured thermodynamic parameter, pK^{exp}. The rationale is that, upon membrane insertion, this pK_a^{memb} value, at the last moment while the group is still in contact with solvent and senses the pH value, will define the peptide stability in the membrane-inserted state.

2.5. Analyses and Error Calculations. The thickness of membrane bilayers is often calculated as the distance between the average Z coordinate of the "P" atoms for each monolayer. However, the presence of a peptide may induce local membrane deformations, which will affect these calculations. To circumvent these issues and to quantify membrane perturbations, we developed a method that calculates monolayer thickness values, for different annulus regions in the xy plane moving radially away from the peptide. First, we define an unaffected region, loosely called "bulk", which (in our simulations) corresponds to all "P" atoms beyond a 15 Å radius from pHLIP. The membrane center is then calculated using only these bulk phosphorus atoms as reference. The membrane center allows the splitting of the peptide atoms between the two monolayers, which can now be used in two separate thickness calculations. Moving a sliding annulus (by increasingly changing its radii) away from the peptide in the xy plane (2 dimensions), we calculate the distance between the average "P" atoms (contained in the annulus) Z position and the membrane center. This procedure is applied to all snapshots of our simulations, and, at longer radii, both monolayer thickness values should converge to a "bulk" value, i.e. half the thickness value for pure POPC.

All error values shown in the pK_a profile plots were obtained using a modified jackknife resampling method. We generated 5 subset combinations of our total sampling by using only 4 out of 5 replicates (1234, 1235, 1245, 1345, and 2345). We used these combinations for the slicing and Hill fitting procedure. The final standard errors were calculated using the generalized formula:

$$\mathrm{SE} = \left\{ \frac{n-1}{n} \sum \left(\frac{\bar{x} - x_i}{n-1} \right)^2 \right\}^{1/2} \quad (1)$$

In the equation, n is the number of simulation replicates, $\bar{x}$ is the predicted pK_a value, and x_i is the pK_a value obtained in each i combination of replicates. We also apply the previous criteria to the pK_a values calculation, namely, each i subset requires at least 50 frames for each protonation state and a minimum of two different pH values. Note that this standard error calculation procedure introduces a new restriction criteria to the final pK_a profile plots, where all protonation/insertion values need to be originated from more than one replicate. Finally, all points with error values above 2 pK units were excluded.

2.6. Synthesis of pHLIP. The L16H pHLIP variant was produced by solid-phase synthesis and purified by CS Bio Co. and was characterized by reversed-phase high performance liquid chromatography (RT-HPLC) using Zorbax SB-C18 and Zorbax SB-C8, 4.6 × 250 mm 5 μm columns (Agilent Technologies). Peptide solution concentrations were deter-

DOI: 10.1021/acs.jctc.8b00102
J. Chem. Theory Comput. 2018, 14, 3289−3297

mined using absorbance at 280 nm, where ϵ_{280} = 13940 M^{-1} cm^{-1}.

2.7. Liposome Preparation. Small unilamellar vesicles were used as model membranes and were prepared via thin film formation, rehydration, and extrusion. A thin lipid film was prepared by dissolving 1-palmitoyl-2-oleoyl-*sn*-glycero-3-phosphocholine (POPC; Avanti Polar Lipids) in chloroform at a concentration of 33 mg mL^{-1}, then desolvated using rotary evaporation, and placed under vacuum for 2 h. The resulting thin POPC film was rehydrated using 2 mM citrate-phosphate buffer at pH 8. Finally, the liposome solution was vortexed and extruded 21 times through a membrane with a pore size of 50 nm.

2.8. pH Dependence Measurements. The pH dependence measurements were carried out by monitoring the shift of the position of maximum of peptide fluorescence as a characteristic of changes of the peptide environment by varying pH. Peptide fluorescence spectra were measured using a PC1 spectrofluorometer (ISS) with temperature control set to 25.0 °C. Tryptophan residues were excited using an excitation wavelength of 295 nm. Both excitation and emission slits were set to 4 nm widths; excitation and emission polarizers were set to 54.7° (magic angle) and 0.0°, respectively. Samples were prepared 24 h prior to running experiments to allow for equilibration in State II.

The pH of solutions containing 7 μM peptide and 1.4 mM POPC was lowered using citric acid and measured using an Orion PerHecT ROSS Combination pH Micro Electrode and an Orion Dual Star pH and ISE Benchtop Meter (Thermo Fisher Scientific) before and after spectrum measurement to ensure equilibration. At each pH, the tryptophan fluorescence spectrum was recorded, and the spectra were analyzed using the Protein Fluorescence and Structural Toolkit (PFAST) to determine the positions of spectral maxima.[18] The obtained positions of spectral maxima were plotted as a function of pH. The pH-dependence curve was fit using the Levenberg−Marquardt iteration algorithm of the bidose response module in Origin 2017 to determine parameters of cooperativity and midpoint of the transitions.

2.9. Oriented Circular Dichroism Measurements. Oriented circular dichroism (OCD) measurements were performed on an MOS-450 spectrometer (Bio-Logic Science Instruments) in the range of 190 to 260 nm with a step size of 1 nm and with temperature control set to 25.0 °C. OCD was conducted using supported planar POPC bilayers prepared using a Langmuir−Blodgett system (KSV Nima). Fourteen quartz slides with 0.2 mm spacers were used; after sonicating the slides in 5% cuvette cleaner (Contrad 70; Decon Laboratories) in deionized water (≥18.2 MΩ cm at 25 °C; Milli-Q Type 1 Ultrapure Water System, EMD Millipore) for 15 min and then rinsing with deionized water, the slides were immersed and sonicated for 10 min in 2-propanol, sonicated again for 10 min in acetone, sonicated once more in 2-propanol for 10 min, and rinsed carefully with deionized water. Lastly, the slides were immersed in a 3:1 solution of sulfuric acid to hydrogen peroxide for 5 min and rinsed thoroughly with deionized water. The slides were stored in deionized water until they were used. POPC bilayers were deposited on the 14 slides using a Langmuir−Blodgett minitrough: a 2.5 mg mL^{-1} solution of POPC in chloroform was spread on the subphase (deionized water), and 15 min was allotted for the evaporation of the chloroform, after which the POPC monolayer was compressed to 32 mN m^{-1}. A lipid monolayer was deposited on the slides by drawing them from the subphase, after which a solution of 10 μM peptide and 500 μM of 50 nm POPC liposomes at pH 4 was added to the slides, producing supported bilayer by fusion between the monolayer on the slides and the peptide-laden lipid vesicles. After incubation for 6 h at 100% humidity, the slides were rinsed with buffer solution to remove residual liposomes, and the spaces between the cuvettes were filled with buffer of appropriate pH. Measurements were taken at three points during the experiment: directly after the addition of the peptide/lipid solution (0 h), after the slides were rinsed to remove excess liposomes after the 6 h incubation time (6 h), and after an additional 12-hour incubation time and rinse with buffer (18 h); these measurements were recorded on the MOS-450 spectrometer with sampling times of 1 s at each wavelength.

3. RESULTS AND DISCUSSION

3.1. Molecular Details of Membrane Inserted pHLIP. The main goal of our work is to elucidate the role of titrable residues in the stability of the *wt*-pHLIP membrane-inserted state (State III). Our calculations should correlate with the equilibrium biophysical studies on liposomes, where pH outside and inside of a liposome equilibrates quickly and is considered to be the same at both sides of a lipid bilayer.[65] We carried out simulations, at different pH values (4.0−7.0), with the peptide inserted in a POPC lipid bilayer. Within the time scale of our simulations (100 ns), the peptide is expected to remain stable in the membrane-inserted state (the withdrawal process occurs in a much larger time scale[65]), which allow us to characterize the effect of pH on the membrane-inserted state.

There is a multitude of experimental data regarding the characterization of pHLIP inserted in lipid bilayers.[1−8,65] In particular, the original transmembrane region (residues 9−30[66]) has often been assumed to be conserved with Asp14 and Asp25 inserted in the lipid bilayer. Although, the helical content is conserved in the membrane-inserted state at all simulated pH values (Figure S1 in the Supporting Information), the overall preferred position of the peptide is significantly shifted toward the N-terminus monolayer (Figure 1 and Figure S2). At all pH values, the peptide bends at the membrane/water interface, consistently losing helical content around residues 15−18. Interestingly, the proline residue at the 20th position is not directly involved in this loss of secondary structure. The presence of Arg11 in the N-terminus domain, close to the interface, and the presence of two segments of hydrophobic residues, 21−24 and 26−30, seem to be the main factors determining both the position and orientation of *wt*-pHLIP in the lipid bilayer. At pH 6.0, which is the experimentally observed pK^{exp}, Asp25 is preferably located at the bilayer center, thus not exchanging protons with water. Concomitantly, Asp14 is only partially inserted in the membrane, singling it out as the key proton active residue. Interestingly, the peptide N-terminus is interchanging between the water phase and the water/membrane interface, suggesting that residues 1−13 are either solvated or adsorbed to the membrane. Varying pH leads to slightly different preferred positions for the transmembrane region of pHLIP, where the ionization of Asp14 seems to be the driving factor for the destabilization of the membrane-inserted state. Nevertheless, even at lower pH values, Asp14 is always able to reach water accessible regions and sense the pH value. At the C-terminus, we observe that the four acidic groups (Asp31, Asp33, Glu34, and C-ter) are also titrating, and their preferred positions relative to the membrane center seem to be

DOI: 10.1021/acs.jctc.8b00102
J. Chem. Theory Comput. 2018, 14, 3289−3297

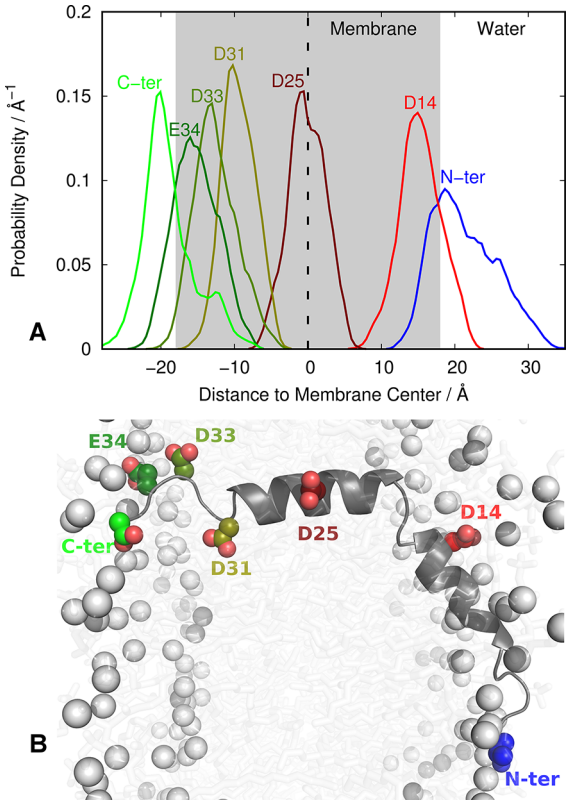

Figure 1. Probability density of distance to membrane center of key titrable groups in *wt*-pHLIP at pH 6.0 (**A**). The membrane region is marked as gray with a dashed line at its center. For the remaining pH values, see Figure S2 of the Supporting Information. Representative conformation of membrane-inserted state of *wt*-pHLIP with the titrable groups highlighted (**B**). Lipid tails are represented as transparent sticks with P atoms as gray spheres. The pHLIP secondary structure is represented as a dark gray cartoon with key titrable groups side chains in spheres.

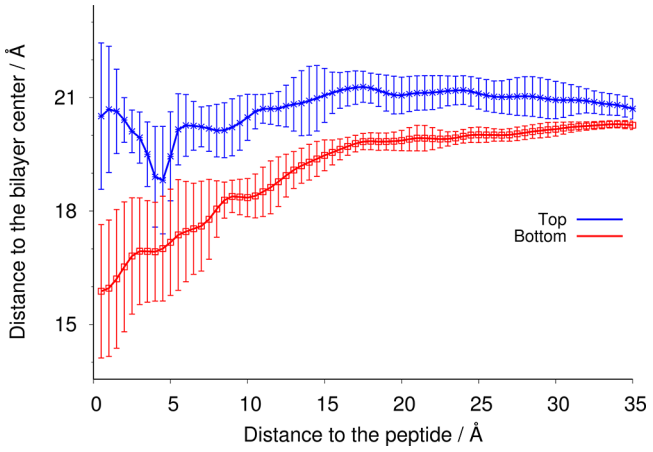

Figure 2. Monolayer thickness profiles for *wt*-pHLIP at pH 6.0. The **Top** monolayer is the one interacting with Asp14, and the **Bottom** monolayer is the one interacting with the C-terminus acidic residues. For the remaining pH values, see Figure S3 of the Supporting Information.

a consequence of their topological order and ionization states. At high pH values, when these residues are mostly ionized, they are not deeply inserted as Figure S2 suggests but rather induce a significant local deformation on the closer monolayer. In fact, the monolayer thickness profiles around pHLIP show a clear local depression in the C-terminus side (Figure 2). A small bilayer deformation (<10%) occurs at pH < 7.0; however, a larger effect is observed at pH 7.0 (~20% − Figure S3 in the Supporting Information), since, at this pH value, the more stable thermodynamic state is not the fully inserted (State III) but rather the membrane-adsorbed (State II). In both cases, the observed deformations are only local being completely dissipated at ~30 Å radially away from the peptide. At the N-terminus side, there is only a small membrane perturbation almost within the error bars. Also, beyond ~15 Å from the peptide, both monolayers thicknesses reach a plateau and the sum of their values corresponds roughly to the experimental POPC thickness (36.5 Å).[67]

3.2. pK_a Profile of Asp14. We calculated the pK_a values of Asp14 using average protonation values obtained from the constant-pH molecular dynamics simulations (CpHMD-L). This method allows for the titrable residues to update their protonation states depending on the pH and their micro-environment. Hence, it is possible to measure the proton affinity of a given group along the membrane normal. Indeed, we have previously observed that aspartic acid, in the middle of a capped alanine pentapeptide (AADAA), has its pK_a value shifted when inserting in a lipid bilayer, favoring its neutral form.[21] The pK_a values, varying with the level of residue insertion into the membrane, can be called pK_a profiles. A key feature of this method is a good estimation of the depth of insertion of a particular residue, which correlates with its solvent exposure, taking into consideration the membrane local deformation. In a pK_a profile, the value calculated at the deepest membrane-inserted location of a residue, the pK_a value at the limit of our sampling, could be considered as an estimation of the pK_a^{memb}. It should correspond to a region of scarce solvent exposure, when the residue does not exchange protons with water anymore, and it is no longer able to sense pH. If we know which residue is responsible for the stability of the peptide membrane-inserted state, then its pK_a^{memb} value is our estimation of the experimental pK^{exp}. The pK_a profile of Asp14 shows a significant shift along the membrane normal, reaching a pK_a^{memb} value of 6.0 ± 0.1, at the deepest membrane-inserted position (Figure 3A), which is in excellent agreement with the experimentally observed pK^{exp} value (6.0[24]).

The C-terminus region of pHLIP has five carboxylic acids, including Asp25. In the membrane-inserted configuration, Asp31, Asp33, Glu34, and C-ter are accessing the solvent on the other side of the bilayer, opposite to Asp14. Therefore, in this configuration, their pK_a profiles are only related to the exit pathway (State III to II transition). In a membrane insertion process of pHLIP, the protonation order of these acidic residues is most likely related to their topological position in the peptide sequence (Figure 1). Furthermore, their pK_a values have contributions from the desolvation effects[21] and the electrostatic repulsion between the negatively charged residues. Hence, the observed trend in the pK_a profiles is in agreement with the expected for an anionic group (Figure 3B). The protonation (charge neutralization) of each residue reduces the local negative potential, decreasing the pK_a shift of the remaining residues when they reach similar insertion values. Consequently, Asp31 pK_a^{memb} is high (despite its lack of sampling) because, at this point, all other carboxylic groups are ionized. On the contrary, C-terminus exhibits a small pK_a shift, since it is measured in the absence of other negative charges. Along these lines, Asp25 would show an even higher pK_a^{memb}

DOI: 10.1021/acs.jctc.8b00102
J. Chem. Theory Comput. 2018, 14, 3289−3297

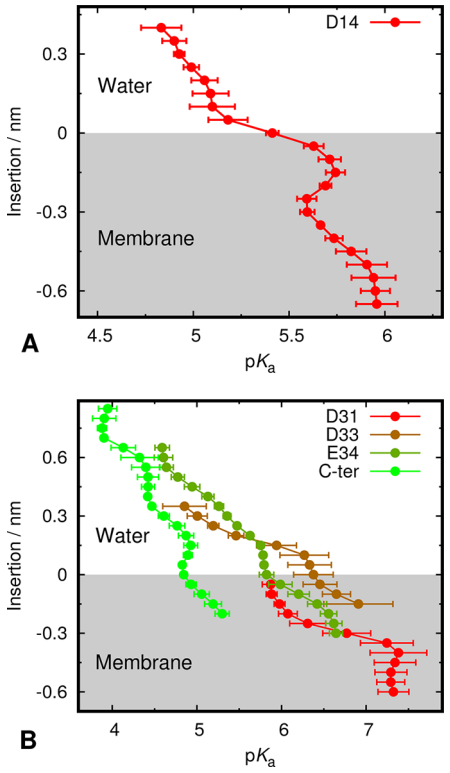

Figure 3. pK_a profile of Asp14 (**A**) and C-terminus acidic residues (**B**) along the membrane normal obtained with CpHMD simulations of *wt*-pHLIP. The negative insertion values correspond to membrane inserted positions, while positive values correspond to more shallow locations. The insertion values were measured between the titrable group and the average position of the selected phosphate groups within a 6 Å radius.

value, but not enough (de)protonation events were observed in our simulations, precluding an accurate pK_a calculation.

pHLIP is in equilibrium between the membrane-adsorbed and membrane-inserted states, and the experimental pK^{exp} value is an average of these populations ratio. According to our results, the occurrence of the membrane-inserted state requires complete protonation of both Asp25 and Asp14, even though the stability of this state is regulated only by the (de)protonation of Asp14, which is able to exchange protons with water. The double protonation is in agreement with isothermal calorimetry (ITC) data, which estimates that 1.8 protons are required for the insertion process.[19] The four carboxylic acids at the C-terminus domain are at the water/membrane interface in both end states, hence, their pK_a values should not have a direct effect on the equilibrium populations. However, the membrane crossing energetic barrier for a charged group is usually unsurmountable.[68,69] Therefore, in the kinetic process of the peptide insertion (or exit) into (from) the membrane, all acidic residues in the C-terminus region would need to, at least transiently, protonate. To obtain a fully neutral C-terminus domain, the acidic groups will likely become neutral sequentially, following their topological order. Hence, these protonations can be slow, depending on the number of anionic residues and their pK_a^{memb} values. This is in agreement with the experimentally observed slow kinetics for *wt*-pHLIP, when compared with other variants with fewer acidic residues in the aforementioned region.[24]

3.3. The L16H Variant Shows Two pK^{exp} Values. The ionization of residues in the pHLIP TM region induces a transition between States III and II. In the *wt*-pHLIP variant, Asp14 preferentially ionizes at pH values larger than 6.0, which leads to the destabilization of the membrane-inserted state and peptide exit from the bilayer. However, below pH 6.0 the peptide membrane-inserted state is well stabilized. By introducing a cationic residue (such as histidine) we observe the opposite effect, i.e. the peptide withdrawal from the membrane now occurs at lower pH values when the residue is ionized.[70] Hence, with a combination of these two strategies, we can design a peptide with two transitions, each having its own pK^{exp} value. In this case, provided that the pK_a^{memb} of the cationic group is lower than that of the anionic, the peptide will be stabilized in its membrane-inserted state in the pH range within the two pK_a^{memb} values (Figure 4). To test this

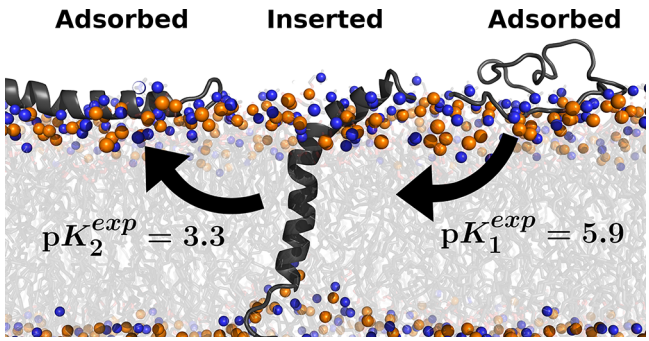

Figure 4. Schematic representation of the pH-dependent mechanism for membrane insertion/withdrawal of L16H pHLIP.

hypothesis, we designed the L16H pHLIP variant, where the cationic residue (His16) is deeply inserted in the membrane and facing an opposite direction from Asp14. We have performed CpHMD simulations with this variant and calculated the corresponding pK_a values (Figure 5). The obtained profiles are similar to the observed for pentapeptides inserting into a lipid bilayer.[21] The pK_a value of His16 (Asp14) decreases (increases) with insertion into the membrane, since the

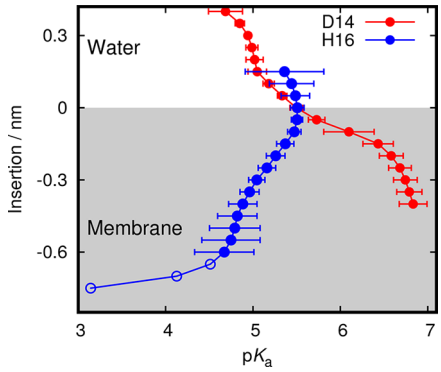

Figure 5. pK_a profiles of Asp14 and His16 along the membrane normal obtained with CpHMD simulations of L16H pHLIP variant. The unfilled circles in the His16 profile correspond to a deep inserted region for which we did not have enough sampling to compute the error bars. They are shown to qualitatively illustrate the profile tendency. The negative insertion values correspond to membrane inserted positions, while positive values correspond to more shallow locations. The insertion values were measured between the titrable group and the average position of the selected phosphate groups within a 6 Å radius. For residues at the C-terminus domain see Figure S4 in the Supporting Information.

DOI: 10.1021/acs.jctc.8b00102
J. Chem. Theory Comput. 2018, 14, 3289−3297

membrane stabilizes their neutral forms. Although the profile of Asp14 is similar to *wt*-pHLIP, we observe a pK_a increase in the membrane-inserted state. This suggests that the histidine residue slightly alters the Asp14 microenvironment upon insertion (even though the conformational properties are not significantly altered - Figures S5 and S6 in the Supporting Information). The two pK_a profiles show that the L16H peptide has two pK_a^{memb} values (6.8 ± 0.2 for Asp14 and 4.7 ± 0.3 - or ∼3.1 without error bars - for His16), thus the peptide is expected to be stabilized in the membrane-inserted state only within the 3.1−6.8 pH range.

The L16H pHLIP variant was synthesized, and its interaction with POPC liposomes was studied employing spectroscopic techniques. The pH-dependence of L16H pHLIP variant was observed by measuring the shift in the peptide fluorescence spectra maximum between pH 1.5 and 8.5 (Figure 6A). The

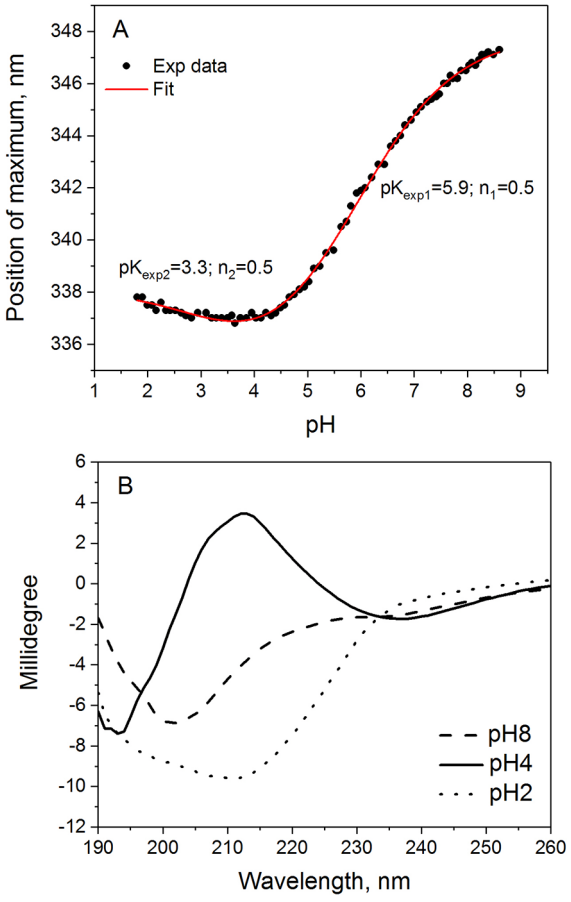

Figure 6. pH-dependence of the position of the maximum shift of Trp fluorescence spectra of L16H pHLIP variant (**A**). The experimental data were fitted using the bidose response module in Origin 2017, to establish cooperativity (n) and mid transition (pK^{exp}). OCD spectra of L16H pHLIP variant measured on POPC-supported bilayers at pH 2, 4, and 8 (**B**).

position of the maximum of the emission spectra mainly reflects the solvent exposure of the tryptophan residues, hence, providing information on the degree of the membrane penetration. The data were fitted assuming two transitions and confirm the existence of two pK^{exp} in L16H pHLIP variant (5.9 and 3.3), which can be attributed to the pK_a^{memb} values of Asp14 and His16, respectively. To identify conformational states of L16H pHLIP at pH 2, 4, and 8 we measured OCD spectra (Figure 6B). At pH 8 no helical structure was observed, while at pH 4 the transmembrane orientation of helix was confirmed. When pH was lowered to 2, the peptide helical content is still preserved. However, contrarily to the observed at pH 4, a surface helical orientation is predominant. Overall, the obtained results support the two-pK_a^{memb} insertion mechanism (Figure 4). Below the lowest pK^{exp}, the His residue in the TM region becomes positively charged, while at a pH value above the highest pK^{exp}, the Asp residue becomes negatively charged. In both cases, it leads to the destabilization of the peptide membrane-inserted state and peptide exit from the bilayer. This inserted state is only stabilized in the pH range between the two pK^{exp} values.

Despite the fact that the membrane-inserted pH range is too wide to be useful for practical applications, the obtained results should be regarded as a proof-of-concept. Hence, they can prompt the design of new pHLIP sequences, with different cationic residues, that might narrow down the pK^{exp} range to ∼1 pH unit, so pHLIP might be able to discriminate between different cells in an organism.

4. CONCLUSIONS

In this work, we studied the protonation profile of all titrable amino acids in two variants of pHLIP peptide when inserted in a lipid bilayer and identified Asp14 as the key residue to act as a sensor of the extracellular pH in the membrane-inserted state. The peptide adopts a preferential position in the membrane such that Asp25 remains mainly at the bilayer center, away from water and unable to sense the pH value, i.e. it is not able to exchange protons with the solvent. The pK_a^{memb} value calculated for Asp14 in *wt*-pHLIP is in excellent agreement with the experimentally measured pK^{exp}. Our simulations also helped to understand the role of the acidic residues at the C-terminus flanking sequence. These residues need to be fully protonated to allow the transition of pHLIP from the membrane-adsorbed (State II) to the membrane-inserted (State III) conformation. Consequently, the number of anionic groups can have a direct influence on the kinetics of the peptide insertion process, as already observed experimentally.[24,65]

The information obtained at the molecular level helped to understand the peptide stability in the membrane and will also give important hints to devise new pHLIP variants with specific features. An example is L16H pHLIP variant, with a histidine residue located in the TM region, near Asp14. Our simulations predicted that this mutation adds a second protonation event, at lower pH values, leading to the peptide withdrawal from the membrane. The simulations were validated by spectroscopic data indicating the presence of two transitions in the L16H pHLIP variant. Although this proof-of-concept mutation seems to generate a too large range between the two pK^{exp} values, it opens an opportunity for the design of new variants to achieve fine-tuning of pH insertion range, hence increasing the potential medical significance of pHLIP technology.

In the future, we also plan to use new enhanced sampling strategies coupled with CpHMD-L simulations in order to improve the accuracy of these pK_a calculations.

■ ASSOCIATED CONTENT

Supporting Information

The Supporting Information is available free of charge on the ACS Publications website at DOI: 10.1021/acs.jctc.8b00102.

DOI: 10.1021/acs.jctc.8b00102
J. Chem. Theory Comput. 2018, 14, 3289−3297

Figures with helicity content, distances to membrane center of key residues, monolayer thickness profiles for both *wt* and L16H variants, and pK_a profile of C-terminus acidic residues of L16H variant (PDF)

AUTHOR INFORMATION

Corresponding Author

*Phone: +351-21-7500112. Fax: +351-21-7500088. E-mail: machuque@ciencias.ulisboa.pt.

ORCID

Miguel Machuqueiro: 0000-0001-6923-8744

Author Contributions

§D.V.-V. and T.F.D.S. contributed equally to this work.

Funding

We acknowledge financial support from Fundação para a Ciência e a Tecnologia through grant SFRH/BPD/110491/2015 and projects UID/MULTI/00612/2013 and PTDC/QEQ-COM/5904/2014. This work was also supported by the General Medical Sciences of the National Institutes of Health grant R01GM073857 to O.A.A. and Y.K.R.

Notes

The authors declare the following competing financial interest(s): O.A.A. and Y.K.R. have founded and have a financial interest in a company, pHLIP, Inc., with the aim of bringing pHLIP technology to the clinic; the company has had no involvement in funding the studies reported here.

ACKNOWLEDGMENTS

We thank Pedro B.P.S. Reis, António M. Baptista, Ana S. Grosso, and Vítor H. Teixeira for fruitful discussions.

REFERENCES

(1) Hunt, J. F.; Rath, P.; Rothschild, K. J.; Engelman, D. M. Spontaneous, pH-dependent membrane insertion of a transbilayer α-helix. *Biochemistry* **1997**, *36*, 15177−15192.

(2) Reshetnyak, Y. K.; Andreev, O. A.; Lehnert, U.; Engelman, D. M. Translocation of molecules into cells by pH-dependent insertion of a transmembrane helix. *Proc. Natl. Acad. Sci. U. S. A.* **2006**, *103*, 6460−6465.

(3) Reshetnyak, Y. K.; Segala, M.; Andreev, O. A.; Engelman, D. M. A monomeric membrane peptide that lives in three worlds: in solution, attached to, and inserted across lipid bilayers. *Biophys. J.* **2007**, *93*, 2363−2372.

(4) Yao, L.; Daniels, J.; Moshnikova, A.; Kuznetsov, S.; Ahmed, A.; Engelman, D. M.; Reshetnyak, Y. K.; Andreev, O. A. pHLIP peptide targets nanogold particles to tumors. *Proc. Natl. Acad. Sci. U. S. A.* **2013**, *110*, 465−470.

(5) Andreev, O. A.; Engelman, D. M.; Reshetnyak, Y. K. Targeting diseased tissues by pHLIP insertion at low cell surface pH. *Front. Physiol.* **2014**, *5*, 97.

(6) Kyrychenko, A.; Vasquez-Montes, V.; Ulmschneider, M. B.; Ladokhin, A. S. Lipid Headgroups Modulate Membrane Insertion of pHLIP Peptide. *Biophys. J.* **2015**, *108*, 791−794.

(7) Hanz, S. Z.; Shu, N. S.; Qian, J.; Christman, N.; Kranz, P.; An, M.; Grewer, C.; Qiang, W. Protonation-Driven Membrane Insertion of a pH-Low Insertion Peptide. *Angew. Chem., Int. Ed.* **2016**, *55*, 12376−12381.

(8) Scott, H. L.; Westerfield, J. M.; Barrera, F. N. Determination of the Membrane Translocation pK of the pH-Low Insertion Peptide. *Biophys. J.* **2017**, *113*, 869−879.

(9) Andreev, O. A.; Karabadzhak, A. G.; Weerakkody, D.; Andreev, G. O.; Engelman, D. M.; Reshetnyak, Y. K. pH (low) insertion peptide (LIP) inserts across a lipid bilayer as a helix and exits by a different path. *Proc. Natl. Acad. Sci. U. S. A.* **2010**, *107*, 4081−4086.

(10) Vasquez-Montes, V.; Gerhart, J.; King, K. E.; Thévenin, D.; Ladokhin, A. S. Comparison of lipid-dependent bilayer insertion of pHLIP and its P20G variant. *Biochim. Biophys. Acta, Biomembr.* **2018**, *1860*, 534−543.

(11) Shu, N. S.; Chung, M. S.; Yao, L.; An, M.; Qiang, W. Residue-specific structures and membrane locations of pH-low insertion peptide by solid-state nuclear magnetic resonance. *Nat. Commun.* **2015**, *6*, 7787.

(12) de Planque, M. R.; Bonev, B. B.; Demmers, J. A.; Greathouse, D. V.; Koeppe, R. E.; Separovic, F.; Watts, A.; Killian, J. A. Interfacial anchor properties of tryptophan residues in transmembrane peptides can dominate over hydrophobic matching effects in peptide- lipid interactions. *Biochemistry* **2003**, *42*, 5341−5348.

(13) Killian, J. A. Synthetic peptides as models for intrinsic membrane proteins. *FEBS Lett.* **2003**, *555*, 134−138.

(14) Vostrikov, V. V.; Daily, A. E.; Greathouse, D. V.; Koeppe, R. E. Charged or aromatic anchor residue dependence of transmembrane peptide tilt. *J. Biol. Chem.* **2010**, *285*, 31723−31730.

(15) Gleason, N. J.; Vostrikov, V. V.; Greathouse, D. V.; Grant, C. V.; Opella, S. J.; Koeppe, R. E. Tyrosine replacing tryptophan as an anchor in GWALP peptides. *Biochemistry* **2012**, *51*, 2044−2053.

(16) Gleason, N. J.; Vostrikov, V. V.; Greathouse, D. V.; Koeppe, R. E. Buried lysine, but not arginine, titrates and alters transmembrane helix tilt. *Proc. Natl. Acad. Sci. U. S. A.* **2013**, *110*, 1692−1695.

(17) Panahi, A.; Brooks, C. L., III Membrane Environment Modulates the pK_a Values of Transmembrane Helices. *J. Phys. Chem. B* **2015**, *119*, 4601−4607.

(18) Shen, C.; Menon, R.; Das, D.; Bansal, N.; Nahar, N.; Guduru, N.; Jaegle, S.; Peckham, J.; Reshetnyak, Y. K. The protein fluorescence and structural toolkit: Database and programs for the analysis of protein fluorescence and structural data. *Proteins: Struct., Funct., Genet.* **2008**, *71*, 1744−1754.

(19) Reshetnyak, Y. K.; Andreev, O. A.; Segala, M.; Markin, V. S.; Engelman, D. M. Energetics of peptide (pHLIP) binding to and folding across a lipid bilayer membrane. *Proc. Natl. Acad. Sci. U. S. A.* **2008**, *105*, 15340−15345.

(20) Musial-Siwek, M.; Karabadzhak, A.; Andreev, O. A.; Reshetnyak, Y. K.; Engelman, D. M. Tuning the insertion properties of pHLIP. *Biochim. Biophys. Acta, Biomembr.* **2010**, *1798*, 1041−1046.

(21) Teixeira, V. H.; Vila-Viçosa, D.; Reis, P. B. P. S.; Machuqueiro, M. pK_a Values of Titrable Amino Acids at the Water/Membrane Interface. *J. Chem. Theory Comput.* **2016**, *12*, 930−934.

(22) Fendos, J.; Barrera, F. N.; Engelman, D. M. Aspartate Embedding Depth Affects pHLIP's Insertion pK_a. *Biochemistry* **2013**, *52*, 4595−4604.

(23) Andreev, O. A.; Dupuy, A. D.; Segala, M.; Sandugu, S.; Serra, D. A.; Chichester, C. O.; Engelman, D. M.; Reshetnyak, Y. K. Mechanism and uses of a membrane peptide that targets tumors and other acidic tissues in vivo. *Proc. Natl. Acad. Sci. U. S. A.* **2007**, *104*, 7893−7898.

(24) Weerakkody, D.; Moshnikova, A.; Thakur, M. S.; Moshnikova, V.; Daniels, J.; Engelman, D. M.; Andreev, O. A.; Reshetnyak, Y. K. Family of pH (low) insertion peptides for tumor targeting. *Proc. Natl. Acad. Sci. U. S. A.* **2013**, *110*, 5834−5839.

(25) Deng, Y.; Qian, Z.; Luo, Y.; Zhang, Y.; Mu, Y.; Wei, G. *Int. J. Mol. Sci.* **2013**, *14*, 14532−14549.

(26) Kong, C. P.; Cui, Y. L.; Zhang, J. L.; Zheng, Q. C.; Zhang, H. X. Mechanism of A pH-induced Peptide Inserting into a POPC Bilayer: A Molecular Dynamic Study. *Curr. Pharm. Biotechnol.* **2014**, *15*, 814−822.

(27) Gupta, C.; Mertz, B. Protonation Enhances the Inherent Helix-Forming Propensity of pHLIP. *ACS Omega* **2017**, *2*, 8536−8542.

(28) Burgi, R.; Kollman, P. A.; van Gunsteren, W. F. Simulating proteins at constant pH: An approach combining molecular dynamics and Monte Carlo simulation. *Proteins: Struct., Funct., Genet.* **2002**, *47*, 469−480.

(29) Lee, M. S.; Salsbury, F. R.; Brooks, C. L., III Constant-pH molecular dynamics using continuous titration coordinates. *Proteins: Struct., Funct., Genet.* **2004**, *56*, 738−752.

DOI: 10.1021/acs.jctc.8b00102
J. Chem. Theory Comput. 2018, 14, 3289−3297

(30) Baptista, A. M.; Teixeira, V. H.; Soares, C. M. Constant-pH molecular dynamics using stochastic titration. *J. Chem. Phys.* **2002**, *117*, 4184−4200.
(31) Dlugosz, M.; Antosiewicz, J. M. Constant-pH molecular dynamics simulations: a test case of succinic acid. *Chem. Phys.* **2004**, *302*, 161−170.
(32) Dlugosz, M.; Antosiewicz, J. M.; Robertson, A. D. Constant-pH molecular dynamics study of protonation-structure relationship in a heptapeptide derived from ovomucoid third domain. *Phys. Rev. E* **2004**, *69*, 021915.
(33) Mongan, J.; Case, D. A.; McCammon, J. A. Constant pH molecular dynamics in generalized Born implicit solvent. *J. Comput. Chem.* **2004**, *25*, 2038−2048.
(34) Machuqueiro, M.; Baptista, A. M. Constant-pH Molecular Dynamics with Ionic Strength Effects: Protonation-Conformation Coupling in Decalysine. *J. Phys. Chem. B* **2006**, *110*, 2927−2933.
(35) Machuqueiro, M.; Baptista, A. M. Molecular Dynamics Constant-pH and Reduction Potential: Application to Cytochrome c_3. *J. Am. Chem. Soc.* **2009**, *131*, 12586−12594.
(36) Itoh, S. G.; Damjanović, A.; Brooks, B. R. pH replica-exchange method based on discrete protonation states. *Proteins: Struct., Funct., Genet.* **2011**, *79*, 3420−3436.
(37) Machuqueiro, M.; Baptista, A. M. Is the prediction of pK_a values by constant-pH molecular dynamics being hindered by inherited problems? *Proteins: Struct., Funct., Genet.* **2011**, *79*, 3437−3447.
(38) Vorobjev, Y. N. Potential of mean force of water-proton bath and molecular dynamic simulation of proteins at constant pH. *J. Comput. Chem.* **2012**, *33*, 832−842.
(39) Swails, J. M.; Roitberg, A. E. Enhancing conformation and protonation state sampling of hen egg white lysozyme using pH replica exchange molecular dynamics. *J. Chem. Theory Comput.* **2012**, *8*, 4393−4404.
(40) Lee, J.; Miller, B. T.; Damjanovic, A.; Brooks, B. R. Constant pH molecular dynamics in explicit solvent with enveloping distribution sampling and Hamiltonian exchange. *J. Chem. Theory Comput.* **2014**, *10*, 2738−2750.
(41) Swails, J. M.; York, D. M.; Roitberg, A. E. Constant pH replica exchange molecular dynamics in explicit solvent using discrete protonation states: implementation, testing, and validation. *J. Chem. Theory Comput.* **2014**, *10*, 1341−1352.
(42) Magalhães, P. R.; Machuqueiro, M.; Baptista, A. M. Constant-pH Molecular Dynamics Study of Kyotorphin in an Explicit Bilayer. *Biophys. J.* **2015**, *108*, 2282−2290.
(43) Vila-Viçosa, D.; Teixeira, V. H.; Baptista, A. M.; Machuqueiro, M. Constant-pH MD simulations of an oleic acid bilayer. *J. Chem. Theory Comput.* **2015**, *11*, 2367−2376.
(44) Santos, H. A.; Vila-Viçosa, D.; Teixeira, V. H.; Baptista, A. M.; Machuqueiro, M. Constant-pH MD simulations of DMPA/DMPC lipid bilayers. *J. Chem. Theory Comput.* **2015**, *11*, 5973−5979.
(45) Reis, P. B.; Vila-Viçosa, D.; Campos, S. R.; Baptista, A. M.; Machuqueiro, M. Role of Counterions in Constant-pH Molecular Dynamics Simulations of PAMAM Dendrimers. *ACS Omega* **2018**, *3*, 2001−2009.
(46) Wallace, J. A.; Shen, J. K. Charge-leveling and proper treatment of long-range electrostatics in all-atom molecular dynamics at constant pH. *J. Chem. Phys.* **2012**, *137*, 184105.
(47) Bennett, W. F. D.; Chen, A. W.; Donnini, S.; Groenhof, G.; Tieleman, D. P. Constant pH simulations with the coarse-grained MARTINI model - Application to oleic acid aggregates. *Can. J. Chem.* **2013**, *91*, 839−846.
(48) Chen, W.; Wallace, J. A.; Yue, Z.; Shen, J. K. Introducing titratable water to all-atom molecular dynamics at constant pH. *Biophys. J.* **2013**, *105*, L15−L17.
(49) Goh, G. B.; Hulbert, B. S.; Zhou, H.; Brooks, C. L., III Constant pH molecular dynamics of proteins in explicit solvent with proton tautomerism. *Proteins: Struct., Funct., Genet.* **2014**, *82*, 1319−1331.
(50) Stern, H. A. Molecular simulation with variable protonation states at constant pH. *J. Chem. Phys.* **2007**, *126*, 164112.
(51) Radak, B. K.; Chipot, C.; Suh, D.; Jo, S.; Jiang, W.; Phillips, J. C.; Schulten, K.; Roux, B. Constant-pH Molecular Dynamics Simulations for Large Biomolecular Systems. *J. Chem. Theory Comput.* **2017**, *13*, 5933−5934.
(52) Schmid, N.; Eichenberger, A. P.; Choutko, A.; Riniker, S.; Winger, M.; Mark, A. E.; Van Gunsteren, W. F. Definition and testing of the GROMOS force-field versions 54A7 and 54B7. *Eur. Biophys. J.* **2011**, *40*, 843−856.
(53) Hess, B.; Kutzner, C.; van der Spoel, D.; Lindahl, E. GROMACS 4: Algorithms for Highly Efficient, Load-Balanced, and Scalable Molecular Simulation. *J. Chem. Theory Comput.* **2008**, *4*, 435−447.
(54) Tironi, I. G.; Sperb, R.; Smith, P. E.; van Gunsteren, W. F. A generalized reaction field method for molecular dynamics simulations. *J. Chem. Phys.* **1995**, *102*, 5451−5459.
(55) Poger, D.; Mark, A. E. On the Validation of Molecular Dynamics Simulations of Saturated and cis-Monounsaturated Phosphatidylcholine Lipid Bilayers: A Comparison with Experiment. *J. Chem. Theory Comput.* **2010**, *6*, 325−336.
(56) Chen, W.; Shen, J. K. Effects of system net charge and electrostatic truncation on all-atom constant pH molecular dynamics. *J. Comput. Chem.* **2014**, *35*, 1986−1996.
(57) Smith, P. E.; van Gunsteren, W. F. Consistent dielectric properties of the simple point charge and extended point charge water models at 277 and 300 K. *J. Chem. Phys.* **1994**, *100*, 3169−3174.
(58) Hess, B. P-LINCS: A Parallel Linear Constraint Solver for Molecular Simulation. *J. Chem. Theory Comput.* **2008**, *4*, 116−122.
(59) Miyamoto, S.; Kollman, P. A. SETTLE: An analytical version of the SHAKE and RATTLE algorithm for rigid water models. *J. Comput. Chem.* **1992**, *13*, 952−962.
(60) Hermans, J.; Berendsen, H. J. C.; van Gunsteren, W. F.; Postma, J. P. M. A Consistent Empirical Potential for Water-Protein Interactions. *Biopolymers* **1984**, *23*, 1513−1518.
(61) Bussi, G.; Donadio, D.; Parrinello, M. Canonical sampling through velocity rescaling. *J. Chem. Phys.* **2007**, *126*, 014101.
(62) Parrinello, M.; Rahman, A. Polymorphic transitions in single crystals: A new molecular dynamics method. *J. Appl. Phys.* **1981**, *52*, 7182−7190.
(63) Rocchia, W.; Sridharan, S.; Nicholls, A.; Alexov, E.; Chiabrera, A.; Honig, B. Rapid grid-based construction of the molecular surface and the use of induced surface charge to calculate reaction field energies: Applications to the molecular systems and geometric objects. *J. Comput. Chem.* **2002**, *23*, 128−137.
(64) Baptista, A. M.; Soares, C. M. Some Theoretical and Computational Aspects of the Inclusion of Proton Isomerism in the Protonation Equilibrium of Proteins. *J. Phys. Chem. B* **2001**, *105*, 293−309.
(65) Karabadzhak, A. G.; Weerakkody, D.; Wijesinghe, D.; Thakur, M. S.; Engelman, D. M.; Andreev, O. A.; Markin, V. S.; Reshetnyak, Y. K. Modulation of the pHLIP transmembrane helix insertion pathway. *Biophys. J.* **2012**, *102*, 1846−1855.
(66) Henderson, R.; Baldwin, J. M.; Ceska, T. A.; Zemlin, F.; Beckmann, E.; Downing, K. H. Model for the structure of bacteriorhodopsin based on high-resolution electron cryo-microscopy. *J. Mol. Biol.* **1990**, *213*, 899−929.
(67) Kučerka, N.; Nieh, M.-P.; Katsaras, J. Fluid phase lipid areas and bilayer thicknesses of commonly used phosphatidylcholines as a function of temperature. *Biochim. Biophys. Acta, Biomembr.* **2011**, *1808*, 2761−2771.
(68) Huang, K.; García, A. E. Free energy of translocating an arginine-rich cell-penetrating peptide across a lipid bilayer suggests pore formation. *Biophys. J.* **2013**, *104*, 412−420.
(69) Lazaridis, T.; Leveritt, J. M.; PeBenito, L. Implicit membrane treatment of buried charged groups: Application to peptide translocation across lipid bilayers. *Biochim. Biophys. Acta, Biomembr.* **2014**, *1838*, 2149−2159.
(70) Barrera, F. N.; Weerakkody, D.; Anderson, M.; Andreev, O. A.; Reshetnyak, Y. K.; Engelman, D. M. Roles of carboxyl groups in the transmembrane insertion of peptides. *J. Mol. Biol.* **2011**, *413*, 359−371.

DOI: 10.1021/acs.jctc.8b00102
J. Chem. Theory Comput. 2018, 14, 3289−3297